Coherent superposition of states in degenerate systems using zero-area pulses

M. Saadati-Niari and M. Amiri

Department of Physics, Faculty of Sciences, University of Mohaghegh Ardabili, P.O. Box 179, Ardabil, Iran.

Received 22 June 2023; accepted 29 August 2023

The coherent superposition of states in degenerate quantum systems is investigated using detuned laser pulses in which the Rabi frequencies are time-dependent, and the pulse area is zero. In this study, a quantum system with an arbitrary number of degenerate states in the ground set as well as an arbitrary number of degenerate states in the exciting set is considered. We assume that all states in the ground set are coupled to the excited states using laser pulses such that the pulse area of Rabi frequency is zero, and all of them have the same time dependence. It is also assumed that all laser pulses are in a non-resonant condition with Bohr transitions, and all detunings are the same. We show that by applying the appropriate temporal dependence for the pulses and the appropriate rate for the detunings, the population can be transferred from an arbitrary superposition from the ground states to a desired superposition from the excited states.

Keywords: Population transfer; Morris-Shore transformation; zero pulse; coherent superposition.

DOI: https://doi.org/10.31349/RevMexFis.70.011303

1. Introduction

According to advances in laser fabrication, the coherent transmission of atomic states using laser pulses has been considered in recent decades. The most prominent quantum optics techniques to create coherent population transfer are stimulated Raman adiabatic passage (STIRAP) [1–6], Stark-chirped rapid adiabatic passage (SCRAP) [7–9], and π-pulse [10, 11] techniques. The most straightforward system to study the laser-atom systems is the interaction of a two-level atom with a laser field [10], and also the crucial technique for population transfer in this system is π-pulse method. In this technique, the frequency of laser pulses must be in exact resonance with the corresponding Bohr transition frequency. This technique has been used for many years in various branches of quantum physics such as nuclear magnetic resonance [12], atomic coherence excitation [13], quantum information theory [14], and recently in nuclear-state population transfer [15–17]. The main problem of π-pulse method is that this technique is sensitive to the exact resonance conditions as well as the exact pulse area (exact intensity of the laser pulse). In order to solve this problem, the composite pulse method [18–27] has recently been used for population transfer in two-level systems, in which a series of pulses with specific phases are used for optimal population transfer. In this method, along with increasing the number of pulses, the system's sensitivity to changes in laboratory parameters decreases.

In recent years, the creation of coherent superposition of states due to its application in the field of quantum information has been attracted [28–31]. In Ref. [32], a series of pulses with an average 2π area is used to create a coherent superposition of states in multi-lambda quantum systems. The method used in Ref. [32] is employed for the N-pod system and coupled Hilbert space in [33, 34], respectively. In Ref. [35], a tangent-hyperbolic pulse is used to create a coherent superposition of states in the N-pod quantum system. Recently, the digital adiabatic passage technique (DAP) [36] has been used to create a coherent superposition of states in multi-lambda and the N-pod systems [37].

In order to transfer the population in two-level systems by π-pulse method, the pulse area must be a specific value($A = \pi$) so that the population is completely transferred from the ground state to the excited state. In the π-pulse method, the exact resonance condition is one of the main conditions for population transfer, but non-resonant systems are the closest to real systems, so the study of non-resonant systems in quantum optics is critical [38]. In Ref. [39], coherent excitation of a two-state quantum system by pulses of coherent radiation with zero pulse area has been studied, which originally are studied in the context of self-induced transparency [40]. Zero-area pulse belongs to such pulses whose an integral over the time duration of the pulse reaches to a null value, that implies the pulse shape is an odd function, so because of antisymmetric, acting on a two-state system, will produce temporary excitation but will, upon conclusion of the pulse, return all population to the initial state. However, for off-resonant cases, such pulses do have an effect. It has been shown that when a zero-area pulse is combined with a time-varying detuning, it is possible to produce complete population transfer in a robust manner for sufficiently large peak Rabi frequency. In recent years, much research has been done in this field that can be referred to as the study of adiabatic speedup in cutting a spin chain via a zero-area pulse control [41], quantum dynamics of a two-state system induced by a chirped zero-area pulse [42], and time-dependent two-level, models and zero-area pulses [43]. Since such pulse models become an efficient tool for quantum control, researchers are attracted to investigate the properties of this model. Zero-area pulses can be produced by

many techniques, including ultrashort-shaped pulses, beam splitting and recombination, self-induced transparency, and quasistatic magnetic fields [40]. In recent years, Quantum dynamics of a two-state system induced by a chirped zero-area pulse and single-photon hologram of a zero-area pulse have been studied experimentally [42, 44].

In this study, we will investigate population transfer from a superposition of ground state to a superposition of excited state in the non-resonant condition using zero-pulse lasers. Our goal is to explore the extension of the zero pulse technique for complex systems, such as four-level systems. Different types of four-level systems such as diamond, tripod, or ladder systems have been considered by researchers [45], and we will examine the diamond system because of its applications. This kind of system shows rich quantum interference and coherence features; for example, when the symmetry of the system is broken, single and double-dark resonances can be observed [46], and also it can be applied as a model for observing pressure-induced resonances [47] alternatively, at reaching the quantum degeneracy regime by all-optical means [48]. In quantum information literature, we can apply this system in two-qubit quantum logic gates [49]. In order to use the zero-area pulse technique in the mentioned complex systems, the system must first be converted to an equivalent two-state system. For simplification of the system, we have used step-by-step Morris-Shore (MS) [50–52] transformation as the complex system is reduced to a two-level system and several uncoupled states [34]. Moreover, in Ref. [53], MS transformation is used to investigate the degenerate Landau-Zener model, which consists of two degenerate energy levels whose energies vary with time and in the existence of interactions that couple the states of the two levels in the presence of quantum noise. By converting the complex system to a two-level system, the zero-area pulse technique can be applied to the system, and the population can be transferred from an arbitrary coherent superposition of ground states to an arbitrary coherent superposition of excited states. We will show that the coherent superposition of states in a detuned degenerate system using zero-area pulses is possible, and the results in the fidelity study indicate the appropriateness. We also shall demonstrate that the efficiency of population transfer is not sensitive to small changes in laser parameters, including the maximum value of Rabi frequencies and detunings which results in reasonable robustness.

This paper is organized as follows: Population transfer in non-resonant two-level systems is introduced in Sec. 2. In Sec. 3 the coupling pattern, reduction of the primary system to a two-level system using the MS transformation, the design of laser pulses to use zero pulse area technique, and numerical study are described. In Sec. 4, the implementation of proposed model in real physical systems is investigated, and finally the conclusion is summarized in Sec. 5.

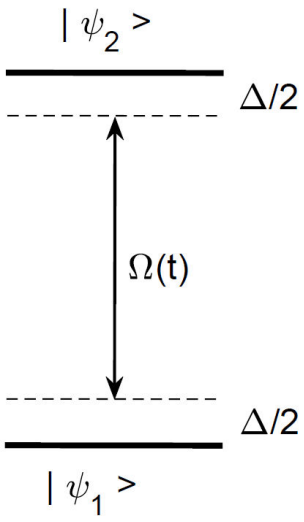

FIGURE 1. Linkage diagram for the two-state system. $\Omega(t)$ is Rabi frequency, the pulse is detuned by Δ from exact resonance and also the Hamiltonian of the system is Eq. (2).

2. Population transfer in non-resonant two-level systems using zero-pulse technique

In order to provide basic concepts in population transfer using zero-area pulses, we provide a summary of the Ref. [39]. According to this reference, we consider the excitation linkage shown in Fig. 1. Coherent excitation of this two-level system is described by the Schrödinger equation, which is mentioned in rotating wave approximation(RWA) as follows [39]:

$$i\hbar\frac{d}{dt}\mathbf{C}(t) = \widehat{H}(t)\mathbf{C}(t), \tag{1}$$

where $\mathbf{C}(t) = [c_1(t), c_2(t)]^T$ is a vector with the amplitude of $c_1(t)$ and $c_2(t)$ that $|c_1(t)|^2$ and $|c_2(t)|^2$ describe the probability of presence in the $|\psi_1\rangle$ and $|\psi_2\rangle$ states respectively, and $\widehat{H}(t)$ is the Hamiltonian of system, which is defined as follows [39]:

$$\widehat{H}(t) = \frac{\hbar}{2}\begin{bmatrix} -\Delta(t) & \Omega(t) \\ \Omega(t) & \Delta(t) \end{bmatrix}, \tag{2}$$

where $\Omega(t)$ is Rabi frequency, indicates the coupling between laser field and states, and $\Delta(t)$ is the offset of the field carrier frequency $\omega(t)$ from the Bohr transition frequency ω_0, $\Delta(t) = \omega(t) - \omega_0$. We assume that the initial state of the system is $|\psi_1\rangle$, and we are interested in transferring the population to the final state $|\psi_2\rangle$. In the case of resonance ($\Delta = 0$) Schrödinger equation can be solved simply, and the probability of transition is $P = \sin^2(A/2)$ which $A = \int \Omega(t)dt$ called pulse area. Complete population transfer occurs when $A = (2n+1)\pi$, which n is a natural number (n=1,2,3,...). According to the transition probability relation, if the pulse area is zero and the system is in exact resonance status, there will be no change in the initial state of the system, at the end of the interaction. In order to implementation of zero-area pulses in

two-level systems, we assume that the Rabi frequency $\Omega(x)$ is an odd function of time as follows [39]:

$$\Omega(x) = -\Omega(-x) = \Omega_0 f(x), \tag{3}$$

where $x = t/T$ represents dimensionless time and $f(x)$ is an odd slow varying and non-oscillating function which is considered as follows [39]:

$$f(x) = \frac{\tanh(x)}{\cosh(x)}. \tag{4}$$

The parameters, Ω_0, Δ and T are assumed to be positive since the transition probability does not depend on their signs. To apply the zero pulse area method in a two-level system, the system is considered in non-resonance condition, and the detuning of the system is constant. First, we calculate the eigenstates of the system, which are called adiabatic states, as follows [39]:

$$|\phi_-(x)\rangle = \cos\upsilon(x)|\psi_1\rangle - \sin\upsilon(x)|\psi_2\rangle, \tag{5a}$$

$$|\phi_+(x)\rangle = \sin\upsilon(x)|\psi_1\rangle + \cos\upsilon(x)|\psi_2\rangle, \tag{5b}$$

where mixing angle is $\upsilon(x) = 1/2\arctan(\Omega(x)/\Delta)$. It can be represented that $|\phi_-(\pm\infty)\rangle = |\psi_1\rangle$ and $|\phi_+(\pm\infty)\rangle = |\psi_2\rangle$, which means initial and final states are equal in the diabatic and adiabatic bases, so a transition in the adiabatic basis describes a transition in the diabatic basis. The Hamiltonian in the basis of adiabatic states can be written as [39]:

$$\widehat{H}(x) = \frac{\hbar}{2}\begin{bmatrix} -\xi(x) & -i\vartheta(x) \\ i\vartheta(x) & \xi(x) \end{bmatrix}, \tag{6}$$

where $\xi(x) = T\sqrt{\Omega^2(x) + \Delta^2}$ and $\vartheta(x) = 2(d/dx)\upsilon(x)$ is nonadiabatic coupling that can be written as follows [39]:

$$\vartheta(x) = \frac{\Delta\Omega_0 f'(x)}{\Delta^2 + \Omega_0^2 f^2(x)}. \tag{7}$$

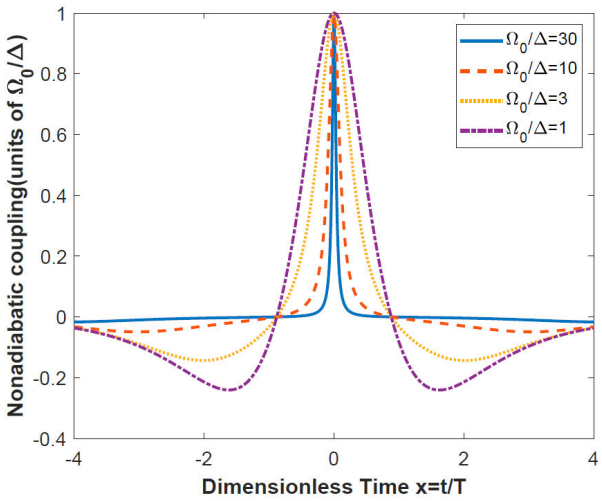

FIGURE 2. Normalized nonadiabatic coupling ($\tilde{\vartheta}(x) = \vartheta(x)/(\Omega_0/\Delta)$) vs the dimensionless time ($x = t/T$) for different values of $\Omega_0/\Delta = 1, 3, 10, 30$. As Ω_0/Δ increases, the central part of $\vartheta(x)$ approaches δ-function behavior.

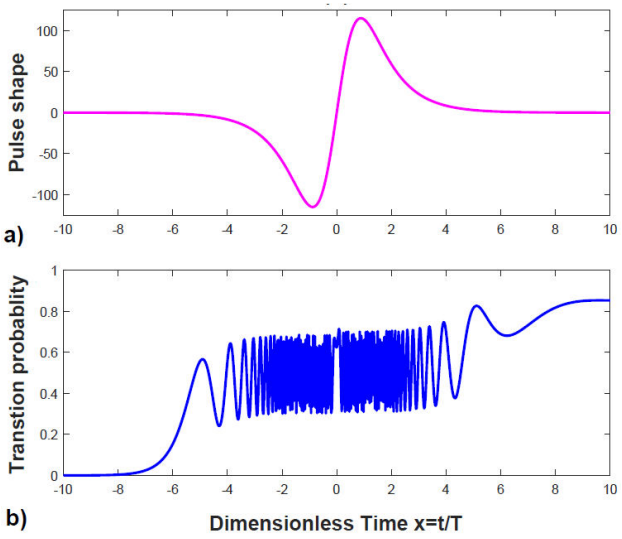

FIGURE 3. Pulse shape $f(x)$ a), the time evolution of the transition probability in diabatic basis b), for the pulse shape (4) with $\Omega_0 T = 250$ and $\Delta T = 2$.

Investigating into nonadiabatic coupling pulse shape in the limit of $\Omega_0/\Delta \to \infty$, shows that the central part of the nonadiabatic coupling Eq. (7) indeed behaves as a δ function with an area of π (see Fig. 2). In the adiabatic basis, the interaction is reduced to the textbook problem of excitation of a two-state system by a δ-function with a peak value of Ω_0/Δ and a pulse area of π. It is observed that in non-resonant condition, population transfer is possible when $\Omega_0 > \Delta$ is fulfilled. Figure 3 illustrates the time evolution of the transition probability in a two-level system for the pulse shape mentioned in Eq. (4), where $\Omega_0 T = 250$ and $\Delta T = 2$.

3. Population transfer in coupled Hilbert space

3.1. The model

A quantum system with N_a states in the lower set $|\psi_m\rangle$ ($m = 1, 2, ..., N_a$) and N_b states in the upper set $|\psi_{N_a+n}\rangle$ ($n = 1, 2, ..., N_b$) is considered. Each of the states in the lower set is coupled to all states in the upper set using time-dependent pulses $\Omega_{mn}(x)$ as displayed in Fig. 4. It should be emphasized that our desired system is the same degenerate system introduced in Ref. [34], with the difference that in Ref. [34], the final reduced system will be a three-level Λ-like system, in which the population will be transferred from a ground state to an arbitrary superposition of other ground states without populating the intermediate states (excited state) by coincident pulses and/or STIRAP techniques. But in this study, the reduced system will be a two-level system that couples the superposition of several ground states to an arbitrary superposition of excited states. Also, in the system introduced in this paper, we consider the non-resonant

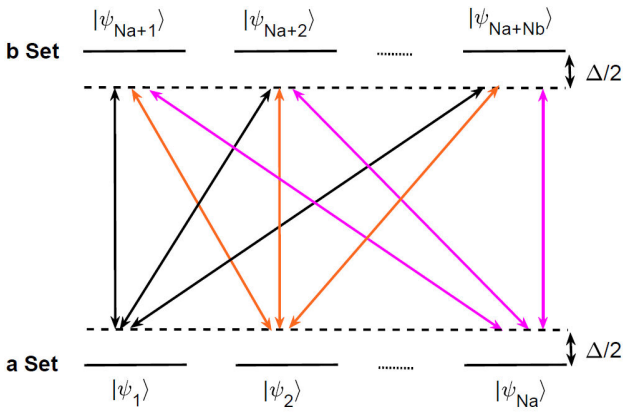

FIGURE 4. A coupled Hilbert system consisting of N_a levels in the ground (a set) and N_b levels in the excited states (b set).

mode and create the desired superposition using zero-area pulses. Also, in the linkage pattern that we have considered in this paper, in order to reduce the initial system to a two-level system, all pulses should have the same time dependence, while in Ref. [34], the time dependence of $\Omega_c^1(x)$ could be different from the time dependence of $\Omega_c^2(x), \Omega_c^3(x), ..., \Omega_c^{N_a}(x)$ pulses. The Hamiltonian of this system is described as:

$$\widehat{H}(x) = \frac{\hbar}{2}\begin{bmatrix} -\Delta I_{N_a} & V \\ V^{\dagger} & \Delta I_{N_b} \end{bmatrix}, \tag{8}$$

where I_{N_a} and I_{N_b} are identity matrices in N_a and N_b dimension respectively, and also V is an $(N_a \times N_b)$-dimensional interaction matrix with time-dependent Rabi frequencies elements,

$$\widehat{V} = \begin{bmatrix} \Omega_{11}(x) & \Omega_{12}(x) & \cdots & \Omega_{1N_b}(x) \\ \Omega_{21}(x) & \Omega_{22}(x) & \cdots & \Omega_{2N_b}(x) \\ \vdots & \vdots & \cdots & \vdots \\ \Omega_{N_a1}(x) & \Omega_{N_a2}(x) & \cdots & \Omega_{N_aN_b}(x) \end{bmatrix}. \tag{9}$$

The initial state of the system is considered as $|\psi(x_i)\rangle = \sum_{i=1}^{N} c_i|i\rangle$ where c_i satisfies $\sum_{i=1}^{N_a} \mid c_i \mid^2 = 1$. We aim to transfer the initial state of the system to an arbitrary coherent superposition of the upper set $|\psi(x_f)\rangle = \sum_{j=1}^{N_b} c'_j|j\rangle$ where $\sum_{j=1}^{N_b} \mid c'_i \mid^2 = 1$ [34].

3.2. Reduction to the two-level system

Since the zero-area pulse technique is used in two-level systems, using two steps of MS transformation, the system introduced in the previous section can be reduced to a two-level system. In the first step, considering time-independent mixing angles θ_j as follows [34]:

$$\frac{\Omega_{12}(x)}{\Omega_{11}(x)} = \frac{\Omega_{22}(x)}{\Omega_{21}(x)} = \cdots = \frac{\Omega_{N_a2}(x)}{\Omega_{N_a1}(x)} = \tan\theta_1, \tag{10a}$$

$$\frac{\Omega_{13}(x)}{\sqrt{\sum_{j=1}^{2}\Omega_{1j}^2(x)}} = \frac{\Omega_{23}(x)}{\sqrt{\sum_{j=1}^{2}\Omega_{2j}^2(x)}} = \cdots = \frac{\Omega_{N_a3}(x)}{\sqrt{\sum_{j=1}^{2}\Omega_{N_aj}^2(x)}} = \tan\theta_2, \tag{10b}$$

$$\vdots$$

$$\frac{\Omega_{1N_b}(x)}{\sqrt{\sum_{j=1}^{N_{b-1}}\Omega_{1j}^2(x)}} = \frac{\Omega_{2N_b}(x)}{\sqrt{\sum_{j=1}^{N_{b-1}}\Omega_{2j}^2(x)}} = \cdots = \frac{\Omega_{N_aN_b}(x)}{\sqrt{\sum_{j=1}^{N_{b-1}}\Omega_{N_aj}^2(x)}} = \tan\theta_{N_{b-1}}. \tag{10c}$$

Considering [34]:

$$\zeta_1 = \prod_{j=1}^{N_b-1}\cos\theta_j, \tag{11a}$$

$$\zeta_2 = \sin\theta_1 \prod_{j=2}^{N_b-1}\cos\theta_j, \tag{11b}$$

$$\vdots$$

$$\zeta_{N_b} = \sin\theta_{N_b-1}, \tag{11c}$$

we can write the corresponding time-independent transformation as [34]:

$$\widehat{T} = \begin{bmatrix} I_a & \mathrm{O} \\ \mathrm{O}^t & T_b \end{bmatrix}, \tag{12}$$

where O is the $(N_a \times N_b)$-dimensional zero matrix and T_b is given by [34]:

$$\widehat{T}_b = \begin{bmatrix} \zeta_1 & \frac{-\zeta_2}{X_2} & \frac{\zeta_1\zeta_3}{X_2X_3} & \cdots & \frac{\zeta_1\zeta_{N_b}}{X_{N_{b-1}}X_{N_b}} \\ \zeta_2 & \frac{\zeta_1}{X_2} & \frac{\zeta_2\zeta_3}{X_2X_3} & \cdots & \frac{\zeta_2\zeta_{N_b}}{X_{N_{b-1}}X_{N_b}} \\ \zeta_3 & 0 & \frac{-X_2^2}{X_2X_3} & \cdots & \frac{\zeta_3\zeta_{N_b}}{X_{N_{b-1}}X_{N_b}} \\ \vdots & \vdots & \vdots & \ddots & \vdots \\ \zeta_{N_b} & 0 & 0 & 0 & \frac{-X_{N_{b-1}}^2}{X_{N_{b-1}}X_{N_b}} \end{bmatrix}, \tag{13}$$

where $X_j = \sqrt{\Sigma_{k=1}^{j}\zeta_k^2}$ $(j = 2, 3, ..., N_b)$ and the transformed Hamiltonian $(\widehat{T}^\dagger \widehat{H}(x)\widehat{T})$ is informed in the MS basis as [34]:

$$\widehat{H}_T^{(1)}(x) = \frac{\hbar}{2}\begin{bmatrix} -\Delta & 0 & \cdots & 0 & \Omega_c^{(1)}(x) \\ 0 & -\Delta & \cdots & 0 & \Omega_c^{(2)}(x) \\ \vdots & \vdots & \vdots & \ddots & \vdots \\ 0 & 0 & \cdots & -\Delta & \Omega_c^{(N_a)}(x) \\ \Omega_c^{(1)}(x) & \Omega_c^{(2)}(x) & \cdots & \Omega_c^{(N_a)}(x) & \Delta \end{bmatrix}, \tag{14}$$

with $\Omega_c^{(i)}(x) = \Omega_{j1}(x)/\zeta_1$. The linkage pattern of Hamiltonian Eq. (14) is an N_a-pod system (see Fig. 5) [34].

In the second step, we want to replace N_a-pod system with a two-level system. To produce this simplification, we define new time-independent mixing angles (φ_j) where $< \varphi_j < \pi/2$:

$$\frac{\Omega_C^{(2)}(x)}{\Omega_C^{(1)}(x)} = \tan\varphi_1, \tag{15a}$$

$$\frac{\Omega_C^{(3)}(x)}{\sqrt{\sum_{j=1}^{2}\Omega_C^{(j)}(x)^2}} = \tan\varphi_2, \tag{15b}$$

$$\vdots$$

$$\frac{\Omega_C^{(N_a)}(x)}{\sqrt{\sum_{j=1}^{N_a-1}\Omega_C^{(j)}(x)^2}} = \tan\varphi_{N_a-1}, \tag{15c}$$

taking:

$$\eta_1 = \prod_{j=1}^{N_a-1}\cos\varphi_j, \tag{16a}$$

$$\eta_2 = \sin\varphi_1\prod_{j=2}^{N_a-1}\cos\varphi_j, \tag{16b}$$

$$\vdots$$

$$\eta_{N_b} = \sin\varphi_{N_a-1}, \tag{16c}$$

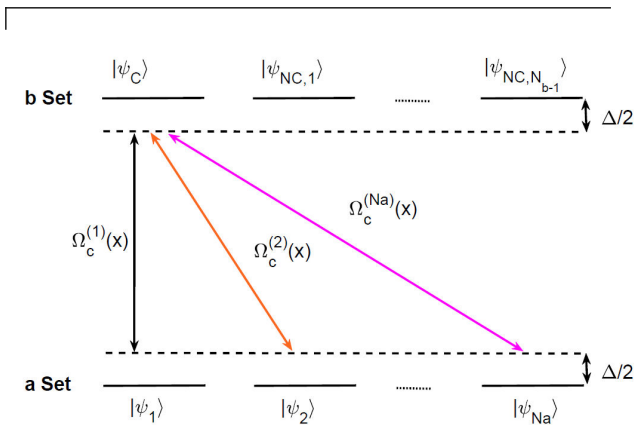

FIGURE 5. Linkage pattern of the multistate system consisting of two coupled sets of levels in the first step MS transformation basis.

following the first step, the corresponding time-independent transformation can be written as:

$$\widehat{T}^2 = \begin{bmatrix} T_{N_a} & \mathrm{O} \\ \mathrm{O}^t & 1 \end{bmatrix}, \tag{17}$$

where T_{N_a} is an N_a-dimensional square matrix that can be obtained by replacing ζ_i with η_i and N_b with N_a in Eq. (13). Finally, corresponding transformed Hamiltonian in $\{\phi_C, \psi_C\}$ subspace is:

$$\widehat{H}_T^{(2)}(x) = (T^{(2)})^\dagger H_T^{(1)} T^{(2)} = \frac{\hbar}{2}\begin{bmatrix} -\Delta & \Omega_c'(x) \\ \Omega_c'(x) & \Delta \end{bmatrix}, \tag{18}$$

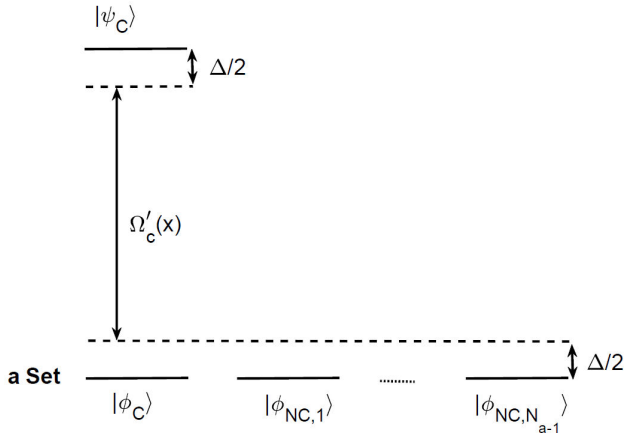

FIGURE 6. Linkage pattern of the multistate system consisting of two coupled sets of levels in the second step MS transformation basis.

where $\Omega'_c(x) = \Omega_c^{(1)}(x)/\eta_1$. Linkage pattern of the multistate system consisting of two coupled sets of levels in the second step MS transformation basis is represented in Fig. 6.

3.3. Example

We consider a quantum diamond system with two states in the ground set and two states in the excited set (see Fig. 7). For this set, the Hamiltonian matrix will be as follows:

$$\widehat{H}(x)=\frac{1}{2}\begin{bmatrix} -\Delta & 0 & \Omega_{11}(x) & \Omega_{12}(x) \\ 0 & -\Delta & \Omega_{21}(x) & \Omega_{22}(x) \\ \Omega_{11}(x) & \Omega_{21}(x) & \Delta & 0 \\ \Omega_{12}(x) & \Omega_{22}(x) & 0 & \Delta \end{bmatrix}. \quad (19)$$

In order to simplify the system, two MS transformation steps will be used. For this purpose, in the first step, the unitary transformation matrix can be obtained using Eq. (13) as follows:

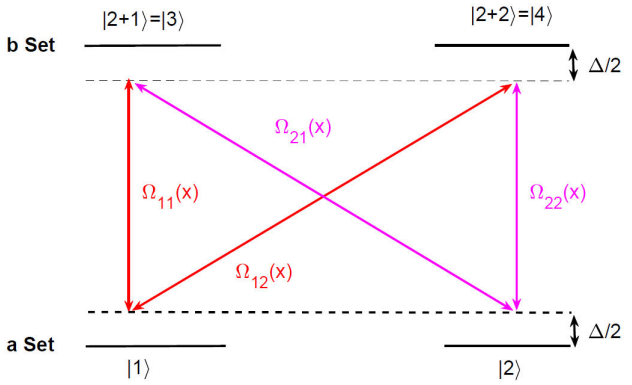

FIGURE 7. The linkage pattern of coupled Hilbert space with two states in the ground and excited levels.

$$\widehat{T} = \begin{bmatrix} 1 & 0 & 0 & 0 \\ 0 & 1 & 0 & 0 \\ 0 & 0 & \cos\theta & -\sin\theta \\ 0 & 0 & \sin\theta & \cos\theta \end{bmatrix}. \quad (20)$$

where:

$$\cos\theta = \frac{\Omega_{11}(x)}{\sqrt{\Omega_{11}^2(x)+\Omega_{12}^2(x)}} = \frac{\Omega_{21}(x)}{\sqrt{\Omega_{21}^2(x)+\Omega_{22}^2(x)}}, \quad (21a)$$

$$\sin\theta = \frac{\Omega_{12}(x)}{\sqrt{\Omega_{11}^2(x)+\Omega_{12}^2(x)}} = \frac{\Omega_{22}(x)}{\sqrt{\Omega_{21}^2(x)+\Omega_{22}^2(x)}}. \quad (21b)$$

The transformed Hamiltonian in the new space is constructed as follows:

$$\widehat{H}_T^{(1)} = \frac{1}{2}\begin{bmatrix} -\Delta & 0 & \Omega_c^{(1)}(x) \\ 0 & -\Delta & \Omega_c^{(2)}(x) \\ \Omega_c^{(1)}(x) & \Omega_c^{(2)}(x) & \Delta \end{bmatrix}. \quad (22)$$

where $\Omega_c^{(1)}(x) = \sqrt{\Omega_{11}^2(x)+\Omega_{12}^2(x)}$ and $\Omega_c^{(2)}(x) = \sqrt{\Omega_{21}^2(x)+\Omega_{22}^2(x)}$. In the second step, in order to use the MS transform, we consider the transformation matrix for transformed Hamiltonian in Eq. (22) as follows:

$$\widehat{T}^{(2)} = \begin{bmatrix} \cos\varphi & \sin\varphi & 0 \\ -\sin\varphi & \cos\varphi & 0 \\ 0 & 0 & 1 \end{bmatrix}, \quad (23)$$

where the mixing angle is $\varphi = \arctan(\Omega_c^{(2)}(x)/\Omega_c^{(2)}(x))$. In this case, as in the previous step, we will have a new Hamiltonian matrix definition:

$$\widehat{H}_T^{(2)} = \frac{1}{2}\begin{bmatrix} -\Delta & \Omega'_c(x) \\ \Omega'_c(x) & \Delta \end{bmatrix}. \quad (24)$$

The coupling parameters will be in the form $\Omega'_c(x) = \sqrt{(\Omega_c^{(1)})^2+(\Omega_c^{(2)})^2}$.

3.4. Pulse design

As previously explained, in order to design the convenient pulse, we consider the initial state of the system as follows:

$$|\psi(x_i)\rangle = \sum_{i=1}^{N_a} c_i|i\rangle, \quad (25)$$

and the final state of the system is

$$|\psi(x_f)\rangle = \sum_{j=1}^{N_b} c'_j|j\rangle. \quad (26)$$

In order to establish the MS conditions, the Rabi frequencies are considered as follows:

$$\Omega_{1j}(x) = c_1 c_j^{'} \Omega_0 g(x), \tag{27a}$$

$$\Omega_{2j}(x) = c_2 c_j^{'} \Omega_0 g(x), \tag{27b}$$

$$\vdots$$

$$\Omega_{N_a j}(x) = c_{N_a} c_j^{'} \Omega_0 g(x), \tag{27c}$$

where $j = 1, 2, ..., N_b$ and $g(x)$ is described as:

$$g(x) = \frac{\tanh(x)}{\cosh(x)}, \tag{28}$$

or

$$g(x) = \frac{x}{(x^2+1)^2}. \tag{29}$$

3.5. Numerical study and robustness

In order to numerical study, we consider a coupled Hilbert space with $N_a = 2$ state in the lower level and $N_b = 2$ in the excited level and impose that the initial state of the system is

$$|\psi(t_i)\rangle = \frac{1}{\sqrt{3}}|1\rangle + \sqrt{\frac{2}{3}}|2\rangle. \tag{30}$$

We aim to transfer the population to the desired state as follows:

$$|\psi(t_f)\rangle = |\psi_{\text{desired}}\rangle = \frac{1}{\sqrt{3}}|3\rangle + \sqrt{\frac{2}{3}}|4\rangle. \tag{31}$$

Figure 8 shows the time evolution of Rabi frequencies, the population, and the fidelity ($F = |\langle\psi(t)|\psi_{\text{desired}}\rangle|^2$) of the desired state. Comparing the final fidelity for the two mentioned type of pulse shapes, it is observed that the final value of the fidelity for the pulse shape, Eq. (28) is 0.9545, and for the pulse shape, Eq. (29) is 0.9755. Figure 7 shows another example for a coupled Hilbert space with $N_a = 2$ and $N_b = 3$ so that the initial state of the system is:

$$|\psi(t_i)\rangle = \frac{1}{\sqrt{2}}(|1\rangle + |2\rangle). \tag{32}$$

and the desired state is:

$$|\psi(t_f)\rangle = |\psi_{\text{desired}}\rangle = \frac{1}{\sqrt{3}}(|3\rangle + |4\rangle + |5\rangle). \tag{33}$$

For this example, we also compared the final fidelity values for the two pulse shapes, and it is observed that this value is 0.9438 for pulse Eq. (28), and 0.9466 for pulse Eq. (29). In order to study the robustness of the zero pulse technique in coupled Hilbert space, we assume that the peak value of Rabi frequencies and detuning deviate from considered values in Fig. 9. Figure 10 shows the contour plot of the final fidelity against Ω_0 and Δ. As observed, if the values of Rabi frequencies and detuning are smaller or more extensive than the considered values, the final fidelity is not significantly affected. We emphasize that in Figs. 8 and 9 we transfer the population from a single ground-state to an arbitrary coherent superposition of excited-states using zero pulse area, which is different from a two-level system where the population is

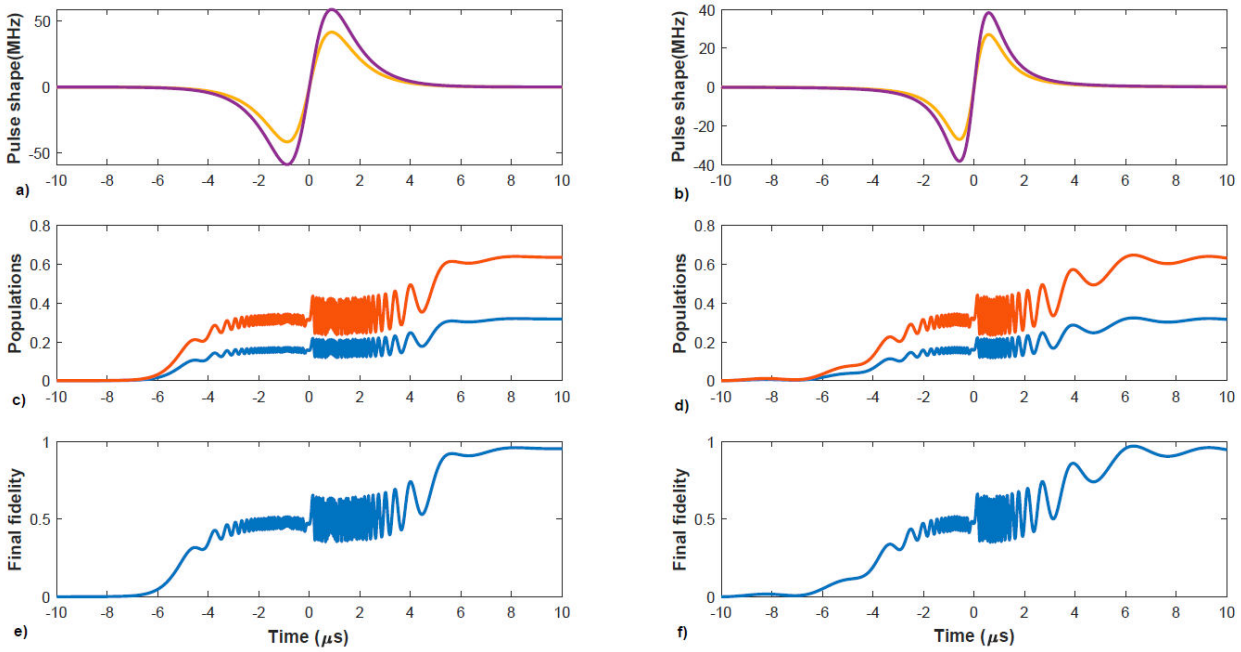

FIGURE 8. Pulse shape a) and b), the time evolution of the population of states c) and d), and final fidelity e) and f) for pulse Eq. (28) and Eq. (29) respectively with the same initial conditions: $\Omega_0 T = 250$ and $\Delta T = 2$.

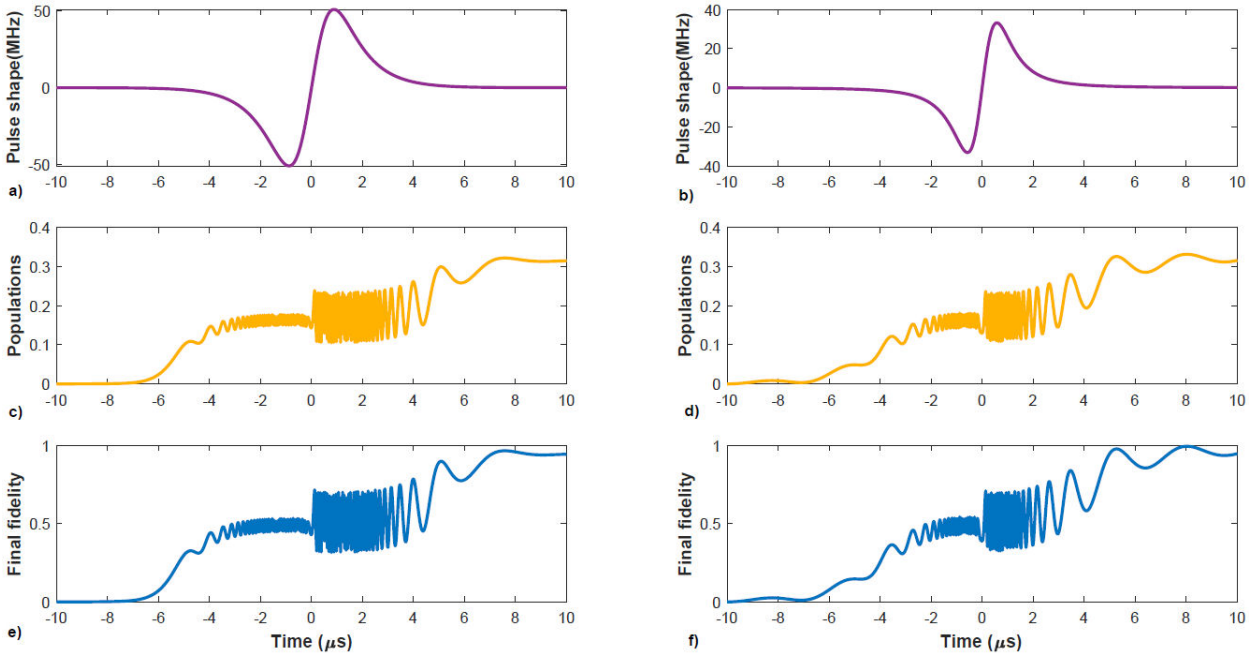

FIGURE 9. Pulse shape a) and b), the time evolution of the population of states c) and d), and final fidelity e) and f) for pulse Eq. (28) and Eq. (29) respectively with the same initial conditions: $\Omega_0 T = 250$ and $\Delta T = 2$.

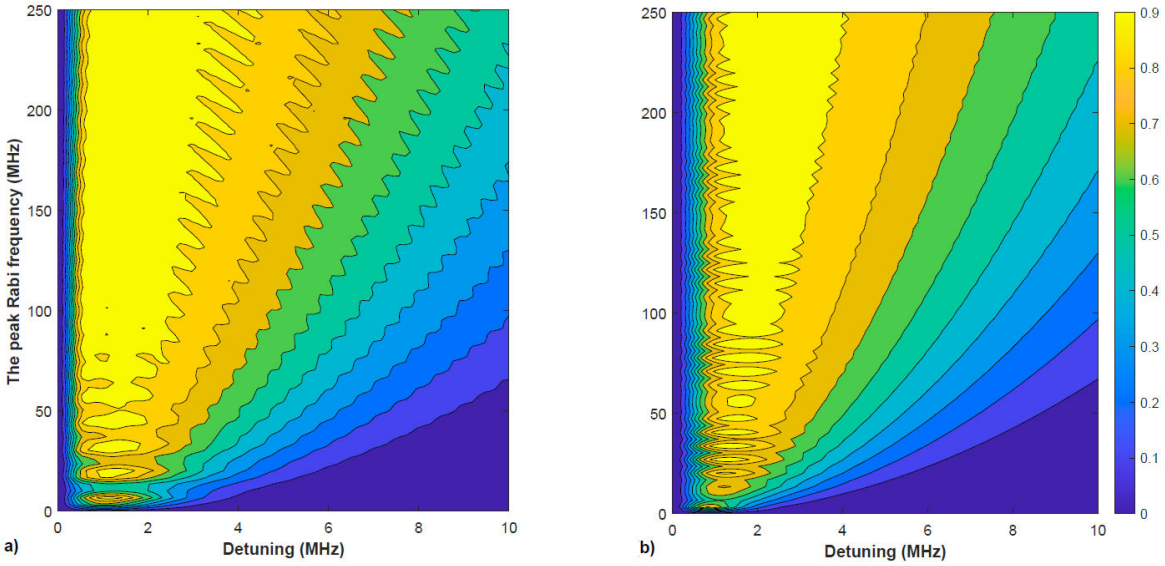

FIGURE 10. Contour plots of the final fidelity as a function of the peak Rabi frequency (Ω_0) and detuning (Δ) for the pulse shape a) Eq. (29), b) Eq. (28).

transferred from a single ground-state to a single excited-state. Coherent superposition of states can be used in various cases, such as the construction of entangled states, quantum gates and quantum algorithms.

4. Implementation in real physical systems

The proposed scheme in this article can be used not only in the case of degenerate systems, but also in the case of non-degenerate systems. For example, consider $J = 0 \leftrightarrow J = 1 \leftrightarrow J = 0$ transition in atomic systems, that is displayed in Fig. 11.

In Fig. 11 The states related to $J = 0$ can be considered as set a and the states related to $J = 1$ considered as the states of set b, and after simplifying the system by using the Morris-Shore transformation, the population from an arbitrary superposition of $J = 0$ states transferred to an arbitrary superposition of $J = 1$ states using zero-area pulses.

Also, our proposed method can be used in nuclear systems as well. Recently, with the progress that has been made in the construction of X-ray lasers, the engineering of nuclear

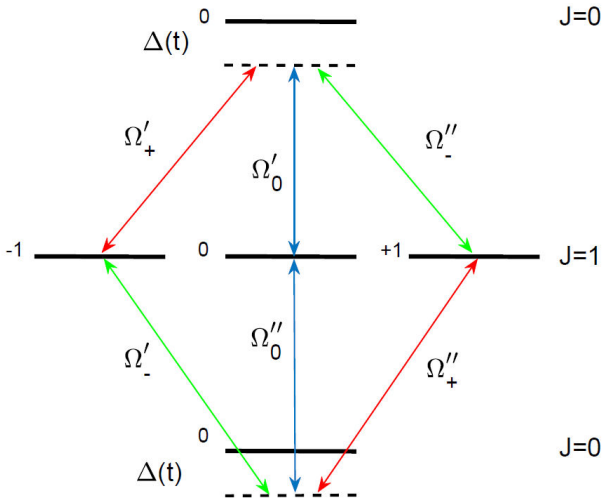

FIGURE 11. Linkage pattern for a three-level ladder involving a degenerate middle level. The two ends of the chain, magnetic sublevels with $J = 0$ have the same detuning from the three intermediate sublevels of $J = 1$.

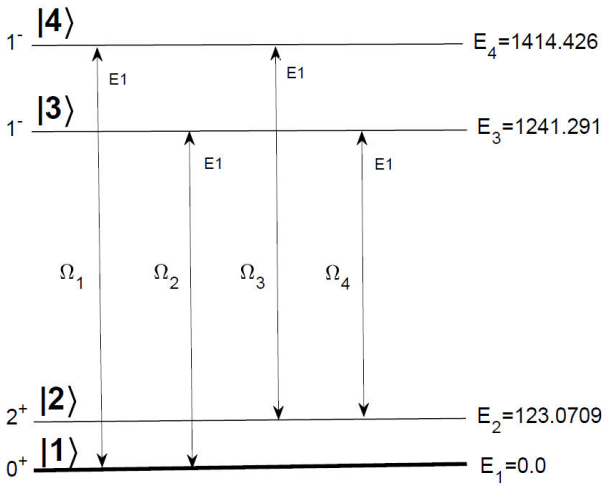

FIGURE 12. Linkage pattern of ^{154}Gd with four X-ray laser pulses in laboratory frame. E_i indicates the energy of the levels and $E1$ indicates the type of electric dipole transition.

states as well as the engineering, of atomic states has been considered [15–17, 54–57]. In nuclear state engineering it is assumed that the accelerated nuclear beam interacts with X-ray laser pulses. Figure 12 shows a linkage pattern of ^{154}Gd nuclei with X-ray laser pulses, which our proposed scheme for zero pulse area can be implemented in this system. In this linkage, all the transitions are related to gamma radiation and each of $|1\rangle$ and $|2\rangle$ states are coupled to $|3\rangle$ and $|4\rangle$ states with two laser pulses. If the system is initially in an arbitrary coherent superposition of $|1\rangle$ and $|2\rangle$ states using the zero-area pulse technique, the population can be transferred to an arbitrary coherent superposition of $|3\rangle$ and $|4\rangle$ states.

Rabi frequencies $\Omega_i (i = 1, 2, 3, 4)$ in nuclear systems depend on the intensity of laser pulses and also the parameters of the nuclei, and considering that the parameters of the nuclei are constant, it is possible to design the Rabi frequencies necessary to use the zero pulse area in nuclear systems by adjusting the shape and intensity of the laser pulses.

5. Conclusion

In this paper, we have studied the coherent superposition of states in a degenerate system using zero-area pulses. To do this, we considered a linkage pattern called the coupled Hilbert space. In the interaction of the laser pulses with the mentioned system, we assumed that all the laser pulses are off-resonance with their corresponding transitions. Besides that, we assumed that all the detunings have the same values. To simplify the Hamiltonian complexity of the system, we used the step-by-step MS transformation to reduce the initial complex system to a two-level system, in which the lower-level and upper-level in MS bases are a superposition of degenerate ground states and degenerate excited states in the original system, respectively. Then we implemented the zero pulse area technique on the reduced two-level system and showed that using this technique in an MS basis, the population can be transferred from one state to another state efficiently, which leads to population transfer from an arbitrary superposition of ground states to an arbitrary superposition of excited states in the original system. In the numerical study of the system's robustness, we showed that the efficiency of population transfer is not sensitive to small changes in laser parameters, including the maximum value of Rabi frequencies and detunings which results in reasonable robustness. Furthermore, we showed that the shape of the pulse does not efficiently influence the final fidelity, although it affects the robustness. The method which is employed in this study can be used to create quantum qudit gates, entangled states, and also to create quantum algorithms that are important in the construction of quantum computers and quantum information theory. Also, our investigation may contribute to the spectroscopy of these systems and the development of new and efficient methods of laser cooling.

Acknowledgments

This work was financially supported by the University of Mohaghegh Ardabili in Iran. The authors would like to thank them for their protection.

1. U. Gaubatz, P. Rudecki, S. Schiemann, K. Bergmann, Population transfer between molecular vibrational levels by stimulated Raman scattering with partially overlapping laser fields. A new concept and experimental results *J. Chem. Phys.* **92** (1990) 5363, https://doi.org/10.1063/1.458514.
2. N. Vitanov, M. Fleischhauer, B.W. Shore, K. Bergmann, Coherent manipulation of atoms molecules by sequential laser pulses *Adv. At. Mol. Opt. Phys.* **46** (2001) 55, https://doi.org/10.1016/S1049-250X(01)80063-X.
3. K. Bergmann, N.V. Vitanov, B.W. Shore, Perspective: Stimulated Raman adiabatic passage: The status after 25 years *J. Chem. Phys.* **142** (2015) 170901, https://doi.org/10.1063/1.4916903.
4. N. V. Vitanov, A. A. Rangelov, B. W. Shore and K. Bergmann, Stimulated Raman adiabatic passage in physics, chemistry, and beyond. *Rev. Mod. Phy.* **89** (2017) 015006, https://doi.org/10.1103/RevModPhys.89.015006.
5. B. W. Shore, Picturing stimulated Raman adiabatic passage: a STIRAP tutorial Advances in Optics and Photonics **9** (2017) 563, https://doi.org/10.1364/AOP.9.000563.
6. K. Bergmann *et al*., Roadmap on STIRAP applications *J. Phys. B* **52** (2019) 202001, https://dx.doi.org/10.1088/1361-6455/ab3995.
7. L. P. Yatsenko *et al.*, Source of metastable H (2s) atoms using the Stark chirped rapid-adiabatic-passage technique *Phys. Rev. A* **60** (1999) R4237, https://doi.org/10.1103/PhysRevA.60.R4237.
8. A. A. Rangelov *et al.*, Stark-shift-chirped rapid-adiabatic-passage technique among three states *Phys. Rev. A* **72** (2005) 053403, https://doi.org/10.1103/PhysRevA.72.053403.
9. N. Shirkhanghah, M. Saadati Niari, and B. Nedaee Shakarab, Stark-shift-chirped rapid-adiabatic-passage technique in tripod systems *Rev. Mex. Fis.* **67.2** (2021) 180, https://doi.org/10.31349/RevMexFis.67.180.
10. L. Allen and J. H. Eberly, Optical Resonance and Two-Level Atoms, (Wiley, New York, 1975).
11. B. W. Shore, The Theory of Coherent Atomic Excitation, (Wiley, New York, 1990).
12. I. Thanopulos, P. Král, M. Shapiro, and E. Paspalakis, Optical control of molecular switches *J. Mod. Opt.* **56** (2009) 686, https://doi.org/10.1080/09500340802326815.
13. K. Bergmann, H. Theuer, B.W. Shore, Coherent population transfer among quantum states of atoms and molecules *Rev. Mod. Phys.* **70** (1998) 1003, https://doi.org/10.1103/RevModPhys.70.1003.
14. F. Vewinger, M. Heinz, R. G. Fernandez, N. V. Vitanov, and K. Bergmann, Creation and measurement of a coherent superposition of quantum states *Phys. Rev. Lett.* **91** (2003) 213001, https://doi.org/10.1103/PhysRevLett.91.213001.
15. T. J. Bürvenich, J. Evers, and C. H. Keitel, Nuclear Quantum Optics with X-Ray Laser Pulses, *Phys. Rev. Lett.* **96** (2006) 142501, https://doi.org/10.1103/PhysRevLett.96.142501.
16. B. Nedaee-Shakarab, M. Saadati-Niari, and F. Zolfagharpour, Nuclear-state population transfer by a train of coincident pulses, *Phys. Rev. C* **94** (2016) 054601, https://doi.org/10.1103/PhysRevC.94.054601.
17. B. Nedaee-Shakarab, M. Saadati-Niari, and F. Zolfagharpour, Nuclear-state engineering in tripod systems using x-ray laser pulses, *Phys. Rev. C* **96** (2017) 044619, https://doi.org/10.1103/PhysRevC.96.044619.
18. B. T. Torosov, E. S. Kyoseva, N. V. Vitanov, Composite pulses for ultrabroadband and ultranarrow-band excitation, *Phys. Rev. A* **92** (2015) 033406, https://doi.org/10.1103/PhysRevA.92.033406.
19. E. S. Kyoseva, N. V. Vitanov, Optimal Quantum Control by Composite Pulses, In CLEO: 2014 (*Optica Publishing Group*, 2014) p. JTu4A.40, https://doi.org/10.1364/CLEO-AT.2014.JTu4A.40.
20. E. Kyoseva, N. V. Vitanov, Arbitrarily accurate passband composite pulses for dynamical suppression of amplitude noise, *Phys. Rev. A* **88** (2013) 063410, https://doi.org/10.1103/PhysRevA.88.063410.
21. B. T. Torosov, N. V. Vitanov, Composite stimulated Raman adiabatic passage, *Phys. Rev. A* **87** (2013) 043418, https://doi.org/10.1103/PhysRevA.87.043418.
22. S. S. Ivanov, A. A. Rangelov, N. V. Vitanov, T. Peters, T. Halfmann, Highly efficient broadband conversion of light polarization by composite retarders, *JOSA A* **29** (2012) 265-269 https://doi.org/10.1364/JOSAA.29.000265.
23. T. Peters *et al*., Variable ultrabroadband and narrowband composite polarization retarders, *Applied optics* **51** (2012) 7466, https://doi.org/10.1364/AO.51.007466.
24. N. V. Vitanov, Arbitrarily accurate narrowband composite pulse sequences, *Phys. Rev. A* **84** (2011) 065404, https://doi.org/10.1103/PhysRevA.84.065404.
25. B. T. Torosov, S. Guérin, N. V. Vitanov, High-Fidelity Adiabatic Passage by Composite Sequences of Chirped Pulses, *Phys. Rev. Lett.* **106** (2011) 233001, https://doi.org/10.1103/PhysRevLett.106.233001.
26. B. T. Torosov, N. V. Vitanov, Smooth composite pulses for high-fidelity quantum information processing, *Phys. Rev. A* **83** (2011) 053420, https://doi.org/10.1103/PhysRevA.83.053420.
27. G. T. Genov, B. T. Torosov, N. V. Vitanov, Optimized control of multistate quantum systems by composite pulse sequences, *Phys. Rev. A* **84** (2011) 063413, https://doi.org/10.1103/PhysRevA.84.063413.
28. G. P. Djotyan *et al.*, Creation of a coherent superposition of quantum states by a single frequency-chirped short laser pulse, *JOSA B* **25** (2008) 2, https://doi.org/10.1364/JOSAB.25.000166.
29. N. Sangouard, S. Guérin, L. P. Yatsenko, and T. Halfmann, Preparation of coherent superposition in a three-state system by adiabatic passage, *Phys. Rev. A* **70** (2004) 013415, https://doi.org/10.1103/PhysRevA.70.013415.
30. E. S. Kyoseva and N. V. Vitanov, Coherent pulsed excitation of degenerate multistate systems: Exact analytic solutions, *Phys. Rev. A* **73** (2006) 023420, https://doi.org/10.1103/PhysRevA.73.023420.

31. M. A. Nielsen and I. Chuang, *Quantum computation and quantum information* (Cambridge University Press, New York, 2001).

32. M. Amniat-Talab, and M. Saadati-Niari, Superposition of states in multi-lambda systems via generalized pulse area method, *J. Mod. Opt.* **61** (2014) 10, https://doi.org/10.1080/09500340.2013.877164.

33. M. Saadati-Niari, and M. Amniat-Talab, Creation of coherent superposition of states in N-pod systems by a train of coincident pulses, *J. Mod. Opt.* **61** (2014) 18, https://doi.org/10.1080/09500340.2014.942404.

34. M. Saadati-Niari, Coherent superpositions of states in coupled Hilbert-space using step by step Morris-Shore transformation, *Ann. Phys.* **372** (2016) 138, https://doi.org/10.1016/j.aop.2016.04.023.

35. S. Mirza-Zadeh, M. Saadati-Niari, and M. Amniat-Talab, Coherent superposition of states in N-pod systems by hyperbolic-tangent coincident pulses, *LaserPhys. Lett.* **15** (2018) 095105, https://doi.org/10.1088/1612-202X/aacfaa.

36. J. A. Vatikus, and A. D. Greentree, Digital three-state adiabatic passage, *Phys. Rev. A* **87** (2013) 063820, https://doi.org/10.1103/PhysRevA.87.063820.

37. N. Irani, M. Saadati-Niari, and M. Amniat-Talab, Digital adiabatic passage in multistate systems, *Physica Scripta.* **95** (2020) 035109, https://doi.org/10.1088/1402-4896/ab4411.

38. D. G. Baranov, A. P. Vinogradov, and A. A. Lisyansky, Abrupt Rabi oscillations in a superoscillating electric field, *Opt. Lett.* **39** (2014) 6316, https://doi.org/10.1364/OL.39.006316.

39. G. S. Vasilev and N. V. Vitanov, Complete population transfer by a zero-area pulse, *Phys. Rev. A* **73** (2006) 023416, https://doi.org/10.1103/PhysRevA.73.023416.

40. W. Bruce, Shore, *Manipulating Quantum Structures Using Laser Pulses* Cambridge University Press, New York, 2011.

41. R.-H. He, R. Wang, F.-H. Ren, L.-C. Zhang, and Z.-M. Wang, Adiabatic speedup in cutting a spin chain via zero-area pulse control, *Phys. Rev. A* **103** (2021) 052606, https://doi.org/10.1103/PhysRevA.103.052606.

42. H.-gyeol Lee, Y. Song, H. Kim, H. Jo, and J. Ahn, Quantum dynamics of a two-state system induced by a chirped zero-area pulse, *Phys. Rev. A* **93** (2016) 023423, https://doi.org/10.1103/PhysRevA.93.023423.

43. J. M. S. Lehto and K.-A. Suominen, Time-dependent two-level models and zero-area pulses, *Physica Scripta* **91** (2015) 013005 https://doi.org/10.1088/0031-8949/91/1/013005.

44. M. Lipka, and M. Parniak, Single-Photon Hologram of a Zero-Area Pulse, *Phys. Rev. Lett* **127** (2021) 163601, https://doi.org/10.1103/PhysRevLett.127.163601.

45. Yi-Chao Li, D. Martínez-Cercós, S. Martínez-Garaot, Xi Chen, and J. G. Muga, Hamiltonian design to prepare arbitrary states of four-level systems, *Phys. Rev. A* **97** (2018) 013830, https://doi.org/10.1103/PhysRevA.97.013830.

46. B.-Q. Ou, L.-M. Liang, C.-Z. Li, Quantum coherence effects in a four-level diamond-shape atomic system, *Opt. Commun* **282** (2009) 2870, https://doi.org/10.1016/j.optcom.2009.03.034.

47. G. Grynberg and P. R. Berman, Pressure-induced extra resonances in nonlinear spectroscopy, *Phys. Rev. A* **41** (1990) 2677, https://doi.org/10.1103/PhysRevA.41.2677.

48. H. Katori, T. Ido, Y. Isoya, and M. Kuwata-Gonokami, Magneto-Optical Trapping and Cooling of Strontium Atoms down to the Photon Recoil Temperature, *Phys. Rev. Lett***82** (1999) 1116, https://doi.org/10.1103/PhysRevLett.82.1116.

49. H. Suchowski, Y. Silberberg, and D. B. Uskov, Pythagorean coupling: Complete population transfer in a four-state system, *Phys. Rev. A* **84** (2011) 013414, https://doi.org/10.1103/PhysRevA.84.013414.

50. J. R. Morris and B. W. Shore, Reduction of degenerate two-level excitation to independent two-state systems, *Phys. Rev. A* **27** (1983) 906, https://doi.org/10.1103/PhysRevA.27.906.

51. A.A. Rangelov, N. V. Vitanov, and B. W. Shore, Extension of the Morris-Shore transformation to multilevel ladders, *Phys. Rev. A* **74** (2006) 053402, https://doi.org/10.1103/PhysRevA.74.053402.

52. B. W. Shore, Two-state behavior in N-state quantum systems: The Morris-Shore transformation reviewed, *J. Mod. Opt.* **61** (2014) 787, https://doi.org/10.1080/09500340.2013.837205.

53. B. Militello, Degenerate Landau-Zener model in the presence of quantum noise, *Int. J. Quantum Inform.* **17** (2019) 1950049, https://doi.org/10.1142/S0219749919500497.

54. W. T. Liao, A. Pálffy, and C. H. Keitel, Nuclear coherent population transfer with X-ray laser pulses, *Phys. Lett. B* **705** (2011) 134, https://doi.org/10.1016/j.physletb.2011.09.107.

55. W. T. Liao, A. Pálffy, and C.H. Keitel, Three-beam setup for coherently controlling nuclear-state population, *Phys. Rev. C* **87** (2013) 054609 https://doi.org/10.1103/PhysRevC.87.054609.

56. N. Mansourzadeh-Ashkani, M. Saadati-Niari, F. Zolfagharpour, and B. Nedaee-Shakarab, Nuclear-state population transfer using composite stimulated Raman adiabatic passage, *Nuclear Physics A* **1007** (2021) 122119, https://doi.org/10.1016/j.nuclphysa.2020.122119.

57. N. Mansourzadeh-Ashkani, M. Saadati-Niari, F. Zolfagharpour, and B., Nedaee-Shakarab, Superposition of nuclear states in multi-lambda systems using x-ray laser pulses, *J. Phys. G: Nucl. Part. Phys.* **49** (2021) 015103, https://doi.org/10.1088/1361-6471/ac3630.